Synthesis, Reactivity, and Electrochemistry of some New Nitrides of Molybdenum and Tungsten: Crystal Structure of Trinuclear $[\{\mu\text{-}MoN(N_3)_2\}\{NMo(N_3)(Et_2PCH_2CH_2PEt_2)_2\}_2]$†

David L. Hughes, Modher Y. Mohammed, and Christopher J. Pickett*
AFRC Institute of Plant Science Research, Nitrogen Fixation Laboratory, University of Sussex, Brighton BN1 9RQ

The reaction between trimethylsilyl azide and *trans*-$[Mo(N_2)_2(depe)_2]$ (depe = $Et_2PCH_2CH_2PEt_2$) gives the mononuclear nitride *trans*-$[MoN(N_3)(depe)_2]$ and also the unexpected linear trinuclear complex $[\{\mu\text{-}MoN(N_3)_2\}\{NMo(N_3)(depe)_2\}_2]$, the structure of which was determined by *X*-ray crystallographic analysis; this, with e.p.r. and electrochemical data, suggests that the trinuclear species is best described as having a localised Mo^{IV},Mo^{V},Mo^{IV} system; protonation and methylation reactions of either the mono- or tri-nuclear nitrides allow the preparation of mononuclear imide derivatives.

We have shown that nitride, imide, and organoimide ligands at mononuclear molybdenum and tungsten have an extensive electrochemistry. For example, a methylimide can be converted into a cyanide[1] [reaction (1), dppe = $Ph_2PCH_2CH_2PPh_2$], certain imides can be directly (or indirectly) reduced under molecular nitrogen to ammonia and dinitrogen complexes[2,3] [reaction (2)], and stepwise oxidation–reduction can provide a pathway for the isomerisation of a methyleneamide to an aminocarbyne ligand[1,4] [reaction (3)].

trans-$[Mo(NMe)Cl(dppe)_2]^+ \longrightarrow$ *trans*-$[Mo(CN)Cl(dppe)_2]$ (1)

trans-$[Mo(NH)Cl(dppe)_2]^+ \longrightarrow$ *trans*-$[Mo(N_2)_2(dppe)_2] + NH_3$ (2)

trans-$[Mo(NCH_2)Cl(dppe)_2] \longrightarrow$ *trans*-$[Mo(CNH_2)Cl(dppe)_2]$ (3)

So that we might extend such ligand-centred electron-transfer chemistry we sought to synthesise electron-rich nitrides and imides. In this paper we describe the preparation, spectroscopic and electrochemical properties of some new molybdenum and tungsten compounds of the basic diphosphine ligand $Et_2PCH_2CH_2PEt_2$, depe, including the novel trinuclear nitride $[\{\mu\text{-}MoN(N_3)_2\}\{NMo(N_3)(depe)_2\}_2]$.

Results and Discussion

Preparation of Complexes.—Chatt and Dilworth[5,6] reported the synthesis of *trans*-$[MoN(N_3)(dppe)_2]$ and showed that it was a convenient precursor to a range of nitride, imide, and alkylimide derivatives. We attempted to prepare *trans*-$[MoN(N_3)(depe)_2]$ by an extension of their method but found that the reaction between *trans*-$[Mo(N_2)_2(depe)_2]$ and $SiMe_3N_3$ gave two metal products, Scheme 1. These were bright yellow *trans*-$[MoN(N_3)(depe)_2]$ (**A**) and orange-brown $[\{\mu\text{-}MoN(N_3)_2\}\{NMo(N_3)(depe)_2\}_2]$ (**B**) which was identified by *X*-ray crystallography as described below.

The formation of the trinuclear compound is favoured by a large excess of the silyl reagent over the starting material, *trans*-$[Mo(N_2)_2(depe)_2]$. A lower ratio favours the formation of (**A**) and this allows optimisation of the yields of (**A**) and (**B**) as described in the Experimental section.

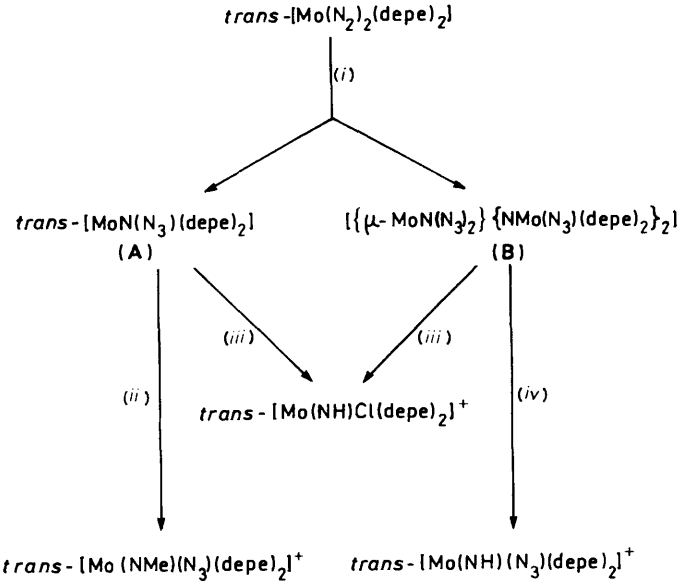

Scheme 1. Pathways for syntheses of nitride and imide complexes of Mo *via* reactions of trimethylsilyl azide with *trans*-$[Mo(N_2)_2(depe)_2]$. (*i*) $SiMe_3N_3$; (*ii*) MeI; (*iii*) HCl; (*iv*) MeOH

We have not studied the mechanism of formation of compound (**B**) but it seems probable that attack of the silyl azide on the primary product *trans*-$[MoN(N_3)(depe)_2]$ gives a Lewis acid to which two additional molecules of (**A**) subsequently ligate, Scheme 2.

The mononuclear nitride (**A**) undergoes straightforward protonation and methylation reactions which parallel those of its dppe analogue: these allow the synthesis of the imide and methylimide derivatives shown in Scheme 1 and described in the Experimental section.

The trinuclear compound also serves as a convenient starting material for mononuclear imides. For example, treatment of (**B**) with HCl gives a chloro-complex and with methanolysis an

† 1,2,2,3-Tetra-azido-1,1,3,3-tetrakis[1,2-bis(diethylphosphino)ethane]-1,2;2,3-di-μ-nitrido-2-nitrido-trimolybdenum.

Supplementary data available: see Instructions for Authors, *J. Chem. Soc., Dalton Trans.*, 1990, Issue 1, pp. xix—xxii.

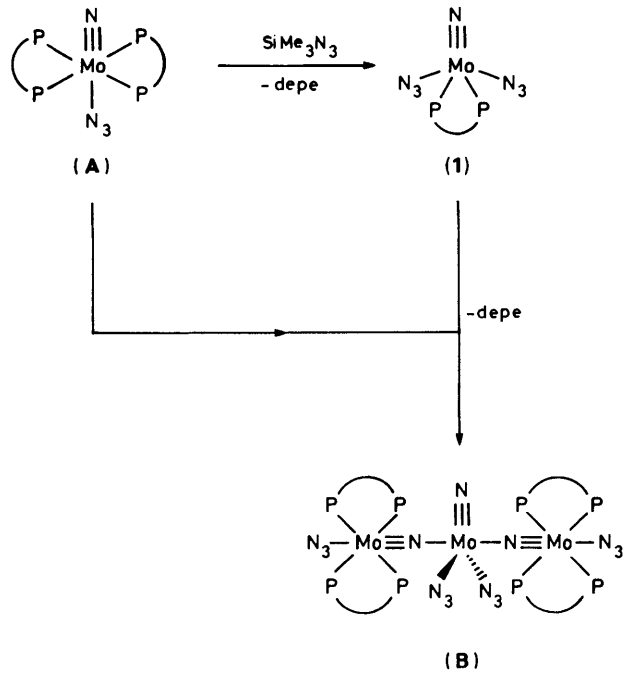

Scheme 2. Proposed pathway for conversion of mononuclear (**A**) into trinuclear (**B**) *via* a molybdenum(v) intermediate (**1**)

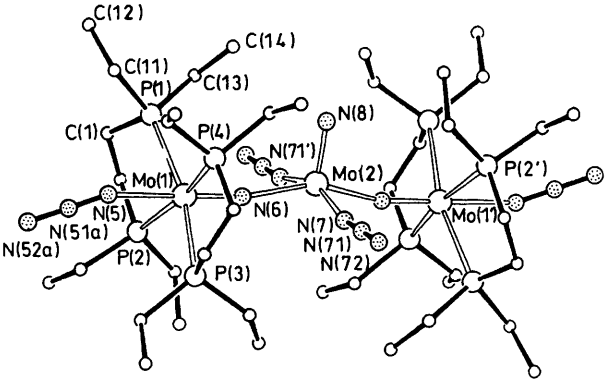

Figure 1. *X*-Ray crystal structure of compound (**B**)

azide, Scheme 1. We have not determined the fate of the central molybdenum moiety but we presume it is the source of hydrazoic acid in the methanolysis reaction.

We have attempted to prepare the tungsten analogues of (**A**) and (**B**) by reactions of *trans*-$[W(N_2)_2(depe)_2]$ with the silyl reagent but without success. However, under forcing conditions we obtain an oil which gives on methanolysis and work-up the imide salt *trans*-$[W(NH)(N_3)(depe)_2][BPh_4]$ in moderate yield, reaction (4).

$$trans\text{-}[W(N_2)_2(depe)_2] \longrightarrow trans\text{-}[W(NH)(N_3)(depe)_2]^+ \quad (4)$$

Microanalytical, spectroscopic, and redox-potential data for the new complexes are listed in Table 1.

The Crystallographic Structure of $[\{\mu\text{-}MoN(N_3)_2\}\{NMo(N_3)(depe)_2\}_2]$.—The linear trinuclear molecule comprises a central square-pyramidal molybdenum(v) unit bridging two octahedral molybdenum(iv) centres, Figure 1. Atomic co-ordinates are listed in Table 2 and selected molecular dimensions in Table 3. In the outer $Mo(depe)_2(N_3)N$ units the two diphosphine ligands form the normal equatorial plane about the Mo(1) atom, with the azido ligand *trans* to the nitride which also bonds the central Mo. These bridging nitrides, N(6) and N(6'), occupy opposite corners of the pyramid base for Mo(2); the other two corners are filled by the azide ligands of N(7) and N(7'), and there is a terminal nitride group in the apical position. In the crystal, these molecules lie disordered about crystallographic centres of symmetry; none of these molecules, of course, can include this symmetry but there is a distribution in the crystal of molecules lying in either one position or its symmetry-related position. The base plane described above and indeed the positions of all the N(7) azide group atoms are the same for either orientation, for the pyramids of Mo(2) or Mo(2'). A similar example of disorder of a square-pyramidal molybdenum complex about a centre of symmetry is found in the anion in crystals of $[PPh_3Me]_2[MoNCl_4]$.[7]

In our complex there is disorder also in the positions of the azide ligands of Mo(1) and in some of the ethyl groups of the depe ligands. Some intra- and inter-molecular contacts appear rather shorter than normal van der Waals distances, but these involve pairs of part-occupied sites, *e.g.* C(42x) ··· N(8) 3.05(6) Å, both of which are unlikely to be occupied in any particular molecule. Thus the orientation of one molecule, *i.e.* which of N(8) or N(8') is occupied, will determine which of the adjacent disordered ethyl group sites will be occupied and, in turn, which of the disordered ethyl group sites in neighbouring molecules will be occupied. The disorder in the N(5) azide groups does not appear to be related directly to such steric effects since none of the atoms is involved in any short interligand or intermolecular contact.

The variations in molybdenum–ligand bond lengths reflect the different oxidation states of the metal atoms and their different co-ordination patterns. Thus, for the azide ligands, the Mo(1)–N(5) distance is rather longer than Mo(2)–N(7) and Mo(2)–N(7'). Also, the molybdenum–terminal nitride, Mo(2)–N(8), distance is marginally shorter than Mo(1)–N(6); the dimensions for this bridging nitride are as might be expected from those found in the octahedral molybdenum(vi) complex tetramer $[\{MoNCl_3(OPCl_3)\}_4]$, where the Mo–N lengths have mean values 1.660(1) and 2.159(9) Å.[8] Other examples of bridging nitrides, with very similar short and long Mo–N bond lengths, include the $[(dtc)_3Mo^{VI}{\equiv}N{\rightarrow}Mo^{VI}(dtc)_3{\leftarrow}N{\equiv}Mo^{VI}(dtc)_3]^{3+}$ cation (dtc = diethyldithiocarbamate),[9] the cyclic $[\{MoNCl_3(OBu^n{}_2)\}_4]$,[10] and the mixed molybdenum-(v), -(vi) complex anion in $[PPh_4]_2[(Mo_2NCl_9)_2]$.[11]

The outer, Mo(1), unit is very similar to the mononuclear $[MoN(N_3)(dppe)_2]$; except for the anomalous, long molybdenum–nitride distance of 1.79(2) Å in that complex, corresponding dimensions are all very similar in the two molecules.[12]

The bonding of N(6) may be considered analogous to that of the linear imido Mo–NR group in which Mo(2) or Mo(2') corresponds to the R group. In the molybdenum(iv) complex $[Mo(NH)Br(dppe)_2]Br{\cdot}MeOH$ the Mo–N bond length is 1.73(2) Å,[12] and in the molybdenum(vi) complexes $[Mo(NH)Cl_2O(OPEtPh_2)_2]$[13] and $[Mo(NCPh_3)(S_2CNMe_2)_3]BF_4{\cdot}0.7CH_2Cl_2$[14] (the last having seven-fold, pentagonal-bipyramidal co-ordination) the corresponding distances are 1.70(1) and 1.731(2) Å. Allowing for the variation in oxidation state and co-ordination number, our Mo(1)–N(6) length is relatively short and confirms a Mo≡N→Mo linkage.

The Electronic Structure of $[\{\mu\text{-}MoN(N_3)_2\}\{NMo(N_3)(depe)_2\}_2]$.—Trinuclear (**B**) is e.p.r.-active and the solution spectrum recorded at 300 K is shown in Figure 2. The single-line spectrum with $g_{iso} = 1.962$ ($I = 0$) is consistent with an unpaired electron isolated on the central molybdenum(v) atom. The spectrum shows $^{95,97}Mo$(spin $\frac{5}{2}$) hyperfine structure,

Table 1. Analytical, spectroscopic, and redox potential data for new nitride and imide complexes

Complex	Analysis[a]/% C	H	N	I.r. (cm^{-1})[b] Mo≡N	N–H	N_3	^{31}P-{^1H} N.m.r. (p.p.m.)[c]	E[d]/V Reduction	Oxidation
$[\{\mu\text{-}MoN(N_3)_2\}\{NMo(N_3)(depe)_2\}_2]$	36.8 (36.3)	7.4 (7.3)	15.5 (15.8)	946	—	2 052	Silent	−2.10,[e] −3.2	−0.22,[e] +0.02,[f] +0.16,[f] +0.49
trans-$[MoN(N_3)(depe)_2]\cdot 0.5C_6H_5Me$	46.0 (46.2)	8.7 (8.7)	8.9 (9.1)	982	—	2 035	−83.4	—	+0.40
trans-$[Mo(NH)(N_3)(depe)_2][BPh_4]$	60.4 (59.7)	8.0 (7.8)	6.5 (6.3)	—	3 220	2 077	−92.4	−2.29	+0.24
trans-$[Mo(NMe)(N_3)(depe)_2][BPh_4]$	60.6 (60.2)	8.0 (7.9)	5.5 (6.2)	—	—	2 077	−93.7	−2.52	+0.18
trans-$[Mo(NH)Cl(depe)_2][BPh_4]$	59.7 (60.1)	8.0 (7.9)	1.6 (1.6)	—	3 260, 3 163	—	−94.7	−2.33	+0.24
trans-$[W(NH)(N_3)(depe)_2][BPh_4]$	53.9 (54.3)	7.4 (7.1)	5.6 (5.8)	—	3 340	2 084	−109.9	−2.62	+0.16

[a] Calculated values in parentheses. [b] Nujol mull. [c] Chemical shift measured in thf relative to trimethyl phosphite. [d] All values are relative to ferrocenium–ferrocene in thf containing 0.2 mol dm^{-3} $[NBu_4][BF_4]$. Unless otherwise noted [e,f] peak potential (E_p) data are given. [e] Reversible at room temperature, $E^{\circ\prime}$ given. [f] Reversible at −40 °C, $E^{\circ\prime}$ given.

Table 2. Final atomic co-ordinates (fractional $\times 10^4$) for $[\{\mu\text{-}MoN(N_3)_2\}\{NMo(N_3)(depe)_2\}_2]$ with estimated standard deviations (e.s.d.s) in parentheses

Atom	x	y	z	S.o.f.*
Mo(1)	1 294.1(5)	705(1)	2 445.0(7)	
P(1)	487(2)	2 009(3)	2 963(3)	
C(11)	833(7)	3 356(13)	3 701(10)	
C(12)	316(10)	4 009(15)	4 110(14)	
C(13)	−361(8)	2 479(19)	2 108(14)	
C(14)	−358(13)	3 425(21)	1 449(17)	
C(1)	176(10)	1 039(16)	3 718(15)	
C(2)	72(9)	−222(20)	3 444(15)	
P(2)	788(2)	−922(3)	3 193(3)	
C(21)	1 354(7)	−1 673(13)	4 272(9)	
C(22)	1 004(10)	−2 483(17)	4 786(12)	
C(23)	307(12)	−2 272(19)	2 446(13)	
C(24)	823(17)	−3 198(24)	2 401(19)	0.7
C(24x)	−136(41)	−2 887(79)	2 288(52)	0.3
P(3)	2 324(2)	−488(3)	2 345(3)	
C(31)	2 887(8)	−1 395(16)	3 349(11)	
C(32)	3 576(10)	−1 933(21)	3 323(15)	
C(33)	2 147(13)	−1 465(31)	1 340(16)	
C(34)	1 889(25)	−2 418(43)	1 128(34)	0.6
C(34x)	2 594(29)	−1 773(55)	1 172(37)	0.4

Atom	x	y	z	S.o.f.*
C(3)	2 965(9)	708(19)	2 277(16)	
C(4)	2 660(9)	1 769(16)	1 743(14)	
P(4)	1 950(2)	2 433(3)	2 015(2)	
C(41)	1 451(15)	3 418(27)	988(14)	
C(42)	1 737(19)	4 039(35)	465(26)	0.6
C(42x)	1 125(31)	3 440(59)	440(42)	0.4
C(43)	2 364(8)	3 593(13)	2 899(10)	
C(44)	2 975(10)	4 356(18)	2 860(13)	
N(5)	2 071(6)	1 119(10)	3 907(7)	
N(51a)	2 413(13)	876(22)	4 653(20)	0.5
N(52a)	2 745(14)	621(24)	5 419(19)	0.5
N(51b)	2 164(17)	1 115(27)	4 648(27)	0.5
N(52b)	2 311(14)	1 026(23)	5 446(19)	0.5
N(6)	710(4)	403(8)	1 348(6)	
Mo(2)	−37(2)	397(2)	−70(3)	0.5
N(7)	760(7)	235(15)	−489(9)	
N(71)	1 175(9)	398(16)	−755(9)	
N(72)	1 616(12)	570(36)	−1 016(16)	
N(8)	−239(12)	1 906(21)	−253(14)	0.5

* Site occupancy factor, if different from 1.0.

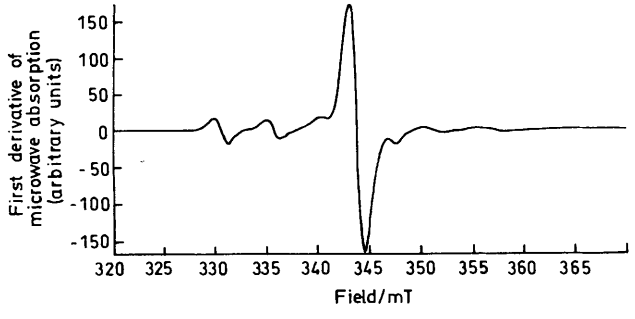

Figure 2. The liquid solution e.p.r. spectrum of compound (**B**) at 300.0 K. The microwave frequency was 9.44 GHz and power 200 mW. The field modulation was 0.1 MT at 100 kHz

A_{iso} = 5.2 mT, associated with this central atom. Additional hyperfine structure which might arise from delocalisation of spin density on to the outer e.p.r.-silent molybdenum(IV) atoms is not observed even in third-derivative spectra: we estimate that spin delocalisation on to the outer Mo atoms, if it occurs, must be less than 20% of that localised on the central Mo^V.

The solution e.p.r. and solid-state *X*-ray data are in accord with compound (**B**) possessing trapped Mo^{IV},Mo^V,Mo^{IV} oxidation states. Further information on the electronic structure of (**B**) with respect to these redox states is provided by the following electrochemical data.

The primary reduction of trinuclear (**B**) is a diffusion-controlled one-electron step at platinum or vitreous carbon electrodes in tetrahydrofuran (thf), dimethylformamide (dmf), or CH_2Cl_2 containing 0.2 mol dm^{-3} $[NBu_4][BF_4]$. Cyclic voltammetry shows this to be a reversible process and that the anion produced is stable for several seconds: a typical voltammogram is shown by Figure 3. The reduction in thf occurs with $E^{\circ\prime}$ at −2.10 V relative to ferrocenium–ferrocene. It is only at extreme potentials in dry solvents that a further reduction is observed: this is an irreversible two-electron

Table 3. Selected molecular dimensions. Bond lengths are in Å, angles in ° with e.s.d.s in parentheses

(*a*) About the Mo atoms

Mo(1)–P(1)	2.496(4)	Mo(2)···Mo(2′)	0.877(5)
Mo(1)–P(2)	2.508(4)	Mo(2)–N(6)	2.153(9)
Mo(1)–P(3)	2.501(4)	Mo(2)–N(6′)	2.122(9)
Mo(1)–P(4)	2.507(4)	Mo(2)–N(7)	1.956(14)
Mo(1)–N(5)	2.268(11)	Mo(2)–N(7′)	2.069(15)
Mo(1)–N(6)	1.701(8)	Mo(2)–N(8)	1.666(22)
P(1)–Mo(1)–P(2)	79.3(1)	N(6)–Mo(2)–N(6′)	156.3(4)
P(1)–Mo(1)–P(3)	165.1(1)	N(6)–Mo(2)–N(7)	88.7(5)
P(1)–Mo(1)–P(4)	98.4(1)	N(6)–Mo(2)–N(7′)	85.4(5)
P(1)–Mo(1)–N(5)	82.6(3)	N(6)–Mo(2)–N(8)	101.9(8)
P(1)–Mo(1)–N(6)	97.2(3)	N(6′)–Mo(2)–N(7)	89.1(5)
P(2)–Mo(1)–P(3)	99.5(1)	N(6′)–Mo(2)–N(7′)	86.7(5)
P(2)–Mo(1)–P(4)	168.9(1)	N(6′)–Mo(2)–N(8)	101.6(8)
P(2)–Mo(1)–N(5)	86.1(3)	N(7)–Mo(2)–N(7′)	155.0(7)
P(2)–Mo(1)–N(6)	94.1(3)	N(7)–Mo(2)–N(8)	102.2(9)
P(3)–Mo(1)–P(4)	79.9(1)	N(7′)–Mo(2)–N(8)	102.7(9)
P(3)–Mo(1)–N(5)	82.6(3)		
P(3)–Mo(1)–N(6)	97.7(3)		
P(4)–Mo(1)–N(5)	82.9(3)		
P(4)–Mo(1)–N(6)	96.9(3)		
N(5)–Mo(1)–N(6)	179.7(4)		
Mo(1)–N(6)–Mo(2)	169.2(5)	Mo(1)–N(6)–Mo(2′)	167.1(5)

(*b*) In the azide ligands

N(5)–N(51a)	1.133(28)	N(51a)–N(52a)	1.156(28)
N(5)–N(51b)	1.09(4)	N(51b)–N(52b)	1.16(3)
N(7)–N(71)	1.078(16)	N(71)–N(72)	1.122(19)
Mo(1)–N(5)–N(51a)	154.9(14)	N(5)–N(51a)–N(52a)	178.1(29)
Mo(1)–N(5)–N(51b)	146.3(19)	N(5)–N(51b)–N(52b)	173.6(38)
Mo(2)–N(7)–N(71)	165.3(17)	N(7)–N(71)–N(72)	178.8(20)

(*c*) Torsion angles in the depe ligands

P(1)–C(1)–C(2)–P(2)	47.4(20)	P(3)–C(3)–C(4)–P(4)	48.3(19)

The primed atoms are related by the centre of symmetry at the origin, close to Mo(2).

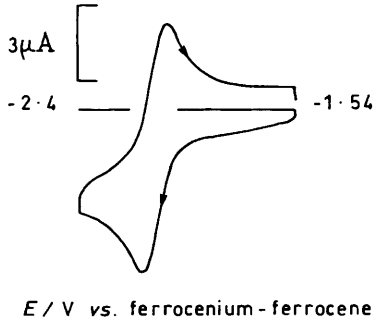

Figure 3. Cyclic voltammetry of compound (**B**) at room temperature in 0.2 mol dm^{-3} $[NBu_4][BF_4]$–thf at a platinum-wire working electrode; the scan rate was 0.2 V s^{-1} with [(**B**)] *ca.* 1 mmol dm^{-3}

process with E_p near −3.2 V *versus* ferrocenium–ferrocene. We associate the primary one-electron reduction with the central, electron-deficient molybdenum(v) centre and this is based on the following arguments.

The outer Mo atoms of compound (**B**) possess a co-ordination sphere quite similar to that of the mononuclear imides *trans*-$[Mo(NH)(N_3)(depe)_2]^+$ and *trans*-$[Mo(NMe)(N_3)(depe)_2]^+$. Therefore, if reduction were localised on the outer Mo atoms we would expect the primary $E°$ for neutral (**B**)

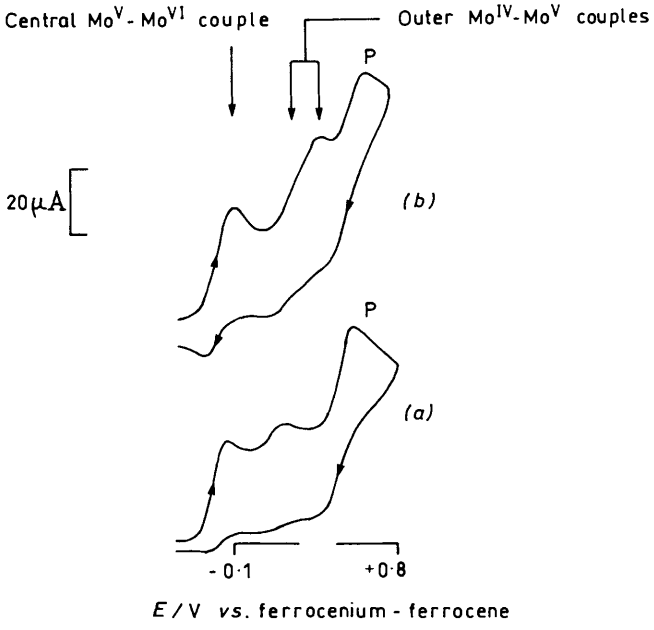

Figure 4. Cyclic voltammetry of compound (**B**) in 0.2 mol dm^{-3} $[NBu_4][BF_4]$–CH_2Cl_2 at (*a*) 20 and (*b*) −20 °C. Voltammograms were recorded at a platinum working electrode at a scan rate of 0.1 V s^{-1}. The peak labelled P corresponds to the oxidation of the product generated from unstable ($\mathbf{B}^+$), see text

to be negative of that of the mononuclear imide or methylimide because the latter carry a positive charge. We find the reverse to be true, (**B**) is substantially easier to reduce than either of these cations (Table 1).

Furthermore, if reduction involved the outer molybdenum(IV) centres then we would expect to observe two reduction processes with a separation in $E°'$ potentials of not more than a few hundred millivolts: the magnitude of the separation would be dependent upon the degree of transmission of electronic effects from one outer Mo atom through the central NMoN to the other (unreduced) Mo atom. That we observe a single reversible one-electron process is inconsistent with isoenergetic reduction orbitals located on the outer Mo atoms.

As discussed above, the e.p.r. data show that the unpaired electron in compound (**B**) is in an orbital essentially localised on the central Mo^V, an electron-deficient 15-electron centre. It seems likely therefore that the reversible addition of an electron involves this half-filled orbital or a superadjacent unoccupied level. Although a localised Mo^V–Mo^{IV} redox step provides the simplest interpretation of data, we cannot exclude the possibility that the redox orbital is one delocalised over the MoNMoNMo framework.

Electrochemical oxidation of trinuclear (**B**) is complicated at normal temperatures but is substantially simplified at −20 °C as the voltammograms of Figure 4(*a*) and (*b*) illustrate. The primary oxidation process is a partially reversible one-electron step which produces an unstable cation ($\mathbf{B}^+$) which at ambient temperature rapidly decomposes to a secondary electroactive product (**P**), Figure 4(*a*). At the lower temperature the decomposition of the cation ($\mathbf{B}^+$) is retarded and this has two consequences on the voltammetry. First, the peak associated with the oxidation of (**P**) is suppressed because less of (**P**) is formed. Secondly, the two overlapping waves which arise from the stepwise oxidation of ($\mathbf{B}^+$) are enhanced because the rate of removal of this species from the diffusion layer by chemical reaction is decreased, Figure 4(*b*).

The overlapping redox system detected in the voltammetry is typical for a complex which possesses two identical redox

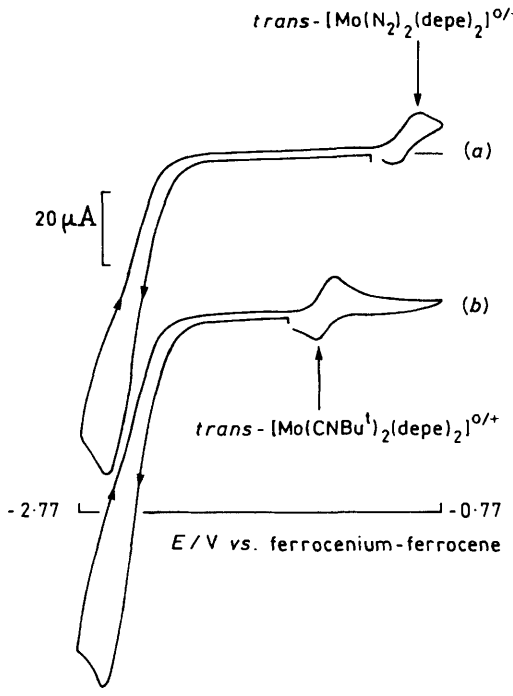

Figure 5. Cyclic voltammetry of *trans*-[Mo(NMe)(N_3)(depe)$_2$] (*ca.* 1 mmol dm^{-3}) in thf–0.2 mol dm^{-3} [NBu_4][BF_4] using a vitreous carbon working electrode and a scan rate of 0.2 V s^{-1}. (*a*) Shows the reduction of the complex under 1 atm (*ca.* 10^5 Pa) of dinitrogen in the presence of *ca.* 10 mmol dm^{-3} PhOH with the detection at *ca.* −1 V of the product *trans*-[Mo(N_2)$_2$(depe)$_2$]. (*b*) Shows the detection of *trans*-[Mo(CNBu^t)$_2$(depe)$_2$] formed upon reduction of the methylimide in the presence of *ca.* 100 mmol dm^{-3} Bu^{t}NC under an atmosphere of argon

centres that are joined by a bridging ligand. We can therefore assign the primary reversible one-electron oxidation to the central Mo^{V}–Mo^{VI} couple and the subsequent $(B)^{+}$–$(B)^{2+}$ and $(B)^{2+}$–$(B)^{3+}$ charge-transfer steps to the outer Mo^{IV}–Mo^{V} couples.

The difference in the standard potentials ΔE for two successive electron-transfer steps involving two identical redox centres within one molecule provides a measure of the electronic interaction between those centres. If such centres are non-interacting, as for example when they are bridged by an insulating group, then ΔE has the statistical value of about 36 mV for monoelectronic steps at 25 °C. We estimate ΔE for $(B)^{+}$ to be about 120 mV and this shows that the outer molybdenum centres are weakly interacting: the removal of the first electron from an outer molybdenum(IV) centre makes the removal of the next electron from the remaining reduced Mo^{IV} slightly more difficult. Delocalisation of the unpaired electron in $(B)^{2+}$ might contribute to the magnitude of ΔE, but it is likely that the electrostatic (field) effect has the dominant influence.

Electrochemistry of the Mononuclear Nitrides and Imides.—Electrochemical studies of oxidation and reduction reactions involving nitrides and imide ligands at the Mo(depe)$_2$ assembly are as yet at a preliminary stage. Nevertheless, voltammetric data have been obtained which allow comparison of redox potentials for the depe complexes with those of related dppe systems and which show that the new complexes have an extensive ligand-centred chemistry.

The primary oxidation potential of the nitride *trans*-[MoN(N_3)(depe)$_2$] (**A**) is about 160 mV negative of that of its dppe analogue. In parallel with this we find that the molybdenum imide complexes *trans*-[Mo(NH)X(depe)$_2$]$^{+}$ (X = Cl or N_3) and *trans*-[W(NH)(N_3)(depe)$_2$]$^{+}$ undergo irreversible reduction at potentials which range from 160 to 260 mV negative of those of their dppe counterparts, Table 1.[2] These data are not unexpected: the greater charge-donating ability of the depe ligand compared with dppe is well recognised and comparable perturbations of redox potentials have been noted elsewhere.[15]

Nonetheless, the nitrido- and imido-complexes are more electron-rich than those hitherto available and they may be useful in developing proton- and electron-transfer chemistry. Here we note that N_2 in complexes of Mo and W ligated by the basic phosphines PMe_3 or depe can be protonated to give an NNH_3 group whereas analogous dppe complexes are not known to protonate beyond the NNH_2 level.[16] At ambient temperatures the nitride *trans*-[MoN(N_3)(depe)$_2$] (**A**) undergoes a diffusion-controlled irreversible oxidation at a platinum electrode in thf containing 0.2 mol dm^{-3} [NBu_4][BF_4]: this process becomes a partially reversible one-electron oxidation at low temperature. The voltammetric behaviour is quite analogous to that of the dppe analogues of (**A**) (M = Mo or W). The irreversibility is directly attributable to the presence of the azide ligand in both depe and dppe complexes because one-electron oxidation of analogous halides gives stable 17-electron cations. We have not identified the product of oxidation of *trans*-[MoN(N_3)(depe)$_2$]; possibly the N_3 ligand breaks down with the release of N_2 leaving an additional nitride ligand at the metal site.

That the imides have ligand-centred reduction chemistry is illustrated by the voltammetry of *trans*-[Mo(NMe)(N_3)(depe)$_2$]$^{+}$ in the presence of phenol as a source of protons with either N_2 or Bu^{t}NC as a co-substrate, Figure 5. The methylimide complex undergoes a multi-electron reduction with the formation of *trans*-[Mo(N_2)$_2$(depe)$_2$] or *trans*-[Mo(Bu^{t}NC)$_2$(depe)$_2$] as illustrated by Figure 5(*a*) and (*b*) respectively. We have shown that the four-electron reduction of *trans*-[Mo(NMe)Cl(dppe)$_2$]$^{+}$ liberates methylamine on reduction at a mercury-pool cathode in the presence of phenol,[2,4] and it is probable that the reduction of *trans*-[Mo(NMe)(N_3)(depe)$_2$]$^{+}$ parallels this chemistry.

Experimental

Crystal Structure Analysis of [{μ-MoN(N_3)$_2$}{NMo(N_3)(depe)$_2$}$_2$].—*Crystal data.* $C_{40}H_{96}Mo_3N_{15}P_8$, M = 1 322.9, monoclinic, space group $P2_1/a$ (equivalent to no. 14), a = 20.280(1), b = 10.712(1), c = 15.414(1) Å, β = 111.587(6)°, U = 3 113.5 Å^3, Z = 2, D_c = 1.411 g cm^{-3}, F(000) = 1 374, μ(Mo-K_α) = 8.2 cm^{-1}, λ(Mo-$K_{\bar{\alpha}}$) = 0.710 69 Å.

Crystals are orange-red plates and slightly air-sensitive. Of several crystals mounted, some were shown not to be single. One crystal, 0.05 × 0.17 × 0.40 mm, coated in epoxy resin, was examined photographically, then transferred to our Enraf-Nonius CAD4 diffractometer (with monochromated radiation) for determination of accurate cell parameters (from the settings of 25 reflections having θ *ca.* 10.5°, each centred in four orientations) and for measurement of diffraction intensities (to $\theta_{max.}$ = 20°). The data were corrected for Lorentz polarisation and absorption effects, for slight deterioration, and to eliminate negative intensities (by Bayesian statistical methods).

2 900 Independent reflections were then input into the SHELX program systems[17] for structure determination and refinement. The automated Patterson routines in SHELXS[18] showed the core of the molecule, the remainder being located in difference Fourier maps. In the refinement process, by full-matrix least-squares methods, it became clear that several parts of the molecule are disordered in the crystal, and each part-atom was refined independently. All the ordered non-hydrogen atoms were allowed anisotropic thermal parameters; the atoms in

partly filled sites were refined isotropically. In the ordered regions of the depe ligands the positions of the methylene H atoms were calculated and their parameters set to ride on those of their bonded C atoms, and the methyl groups were refined as rigid units with the H atoms sharing a common thermal parameter.

At conclusion of refinement, $R = 0.075$, $R' = 0.067$[17] for 2 380 reflections (those with $I \geqslant \sigma_I$), weighted $w = (\sigma_F^2 + 0.001\ 20F^2)^{-1}$. In the final difference map, the highest peaks (*ca.* 0.5 e Å^{-3}) were either in the regions of the disordered ethyl groups or close to the outer Mo atom.

Scattering factors for neutral atoms were taken from ref. 19. Computer programs, including those noted above and listed in Table 4 of ref. 20, used in this analysis were run on the MicroVax II computer in this laboratory.

Additional material available from the Cambridge Crystallographic Data Centre comprises H-atom co-ordinates, thermal parameters, and remaining bond lengths and angles.

Preparation of Complexes.—All reactions were carried out under dry dinitrogen in Schlenk apparatus. Solvents were dried and distilled under dinitrogen before use.

$[\{\mu\text{-}MoN(N_3)_2\}\{NMo(N_3)(depe)_2\}_2]$ (**B**). The complex *trans*-$[Mo(N_2)_2(depe)_2]$[15] (1.19 g, 2.11 mmol) was dissolved in thf (50 cm^3). Trimethylsilyl azide (2.7 cm^3, 20.5 mmol) was added to the solution and the mixture was refluxed for *ca.* 12 h. During this period the solution changed from yellow-orange to dark red. The solvent was removed *in vacuo* and the residue triturated with diethyl ether (40 cm^3). The dark orange solid was removed by filtration, recrystallised from toluene–hexane (1:3), and dried *in vacuo* (yield 0.52 g, 56%).

trans-$[MoN(N_3)(depe)_2]\cdot 0.5C_6H_5Me$ (**A**). The complex *trans*-$[Mo(N_2)_2(depe)_2]$ (0.50 g, 0.89 mmol) was dissolved in thf (50 cm^3). Trimethylsilyl azide (0.5 cm^3, 3.8 mmol) was added and the mixture refluxed for *ca.* 24 h. The solution was taken to dryness and the residue dissolved in the minimum volume of toluene. Hexane was added to precipitate a small amount of the trinuclear complex (**B**) which was removed by filtration over Celite. The filtrate was cooled in liquid nitrogen whereby the product precipitated as a bright yellow solid; it was collected by filtration and dried *in vacuo* (yield 0.26 g, 52%).

trans-$[Mo(NH)Cl(depe)_2][BPh_4]$. The complex *trans*-$[MoN(N_3)(depe)_2]$ (0.42 g, 0.74 mmol) was dissolved in methanol (25 cm^3). Concentrated hydrochloric acid (0.4 cm^3) was added to the solution which changed from yellow to bright red. Sodium tetraphenylborate (0.25 g, 0.74 mmol) was added and the solution stirred for 10 min during which time the product precipitated as a pink crystalline solid. It was removed by filtration, washed with cold methanol, and dried *in vacuo* (yield 0.2 g, 31%).

Essentially the same procedure was used to prepare *trans*-$[Mo(NH)Cl(depe)_2][BPh_4]$ from the trinuclear complex (**B**). Thus this starting material (0.5 g, 0.38 mmol) gave 0.39 g (0.43 mmol) of the imide salt (yield 57%).

trans-$[Mo(NH)(N_3)(depe)_2][BPh_4]$. The trinuclear complex (**B**) (0.30 g, 0.23 mmol) was suspended in methanol (35 cm^3) and the mixture stirred at room temperature overnight. The orange suspension dissolved during this period to give a clear red solution. The addition of $Na[BPh_4]$ (0.16 g, 0.43 mmol) gave the product which crystallised from the methanol as light pink needles. These were filtered off, washed with MeOH, and dried *in vacuo* (yield 0.14 g, 29%).

trans-$[Mo(NMe)(N_3)(depe)_2][BPh_4]$. The complex *trans*-$[MoN(N_3)(depe)_2]$ (1.56 g, 2.8 mmol) was suspended in methanol (30 cm^3), iodomethane (1 cm^3) was added, and the mixture was stirred for *ca.* 1 h. During this period the yellow solid dissolved to give a clear red solution. Sodium tetraphenylborate (1.1 g, 3.2 mmol) was added to give the product as a pink solid. This was removed by filtration, washed with methanol (2 × 4 cm^3), and dried *in vacuo* (yield 1.40 g, 57%).

trans-$[W(NH)(N_3)(depe)_2][BPh_4]$. The complex *trans*-$[W(N_2)_2(depe)_2]$[15] (1.71 g, 1.7 mmol) was dissolved in thf (40 cm^3) and trimethylsilylazide (2 cm^3) was added to the solution. The mixture was refluxed for 24 h with continuous irradiation from two 40-W tungsten lamps. The solvent was removed and the oil triturated with diethyl ether (2 × 50 cm^3). The ether extracts were decanted and discarded. Methanol (60 cm^3) was added to the oily solid and the mixture stirred for 0.5 h. During this period the solid dissolved to give a dark orange-red solution. Sodium tetraphenylborate (0.5 g) was added to the solution which was then stirred for a further 0.5 h. During this period the product formed as an orange-pink microcrystalline solid. It was removed by filtration, washed with methanol (2 × 5 cm^3), and dried *in vacuo* (yield 0.72 g, 44%).

Electrochemical and Spectroscpic Measurements.—Electrochemical measurements were made by cyclic voltammetry at a platinum wire or vitreous carbon disc electrode in 0.2 mol dm^{-3} $[NBu_4][BF_4]$–thf. Methods, materials, and intrumentation have been described elsewhere.[21]

Infrared spectra were recorded on a Bio-Rad FTS-7 Fourier-transform spectrometer and e.p.r. spectra on a Bruker type ER200 D-SRC spectrometer. N.m.r. measurements were made on a JEOL type GSX-270 Fourier-transform spectrometer.

Analytical Data.—Carbon, H, and N analyses were undertaken by Mr. C. J. Macdonald of the Nitrogen Fixation Laboratory, University of Sussex.

Acknowledgements

We thank Dr. D. J. Lowe and Mr. C. J. Macdonald for spectroscopic measurements and valuable discussion, Miss Kaye Cate and Mr. Adrian Hills for experimental assistance, and Miss Beryl Scutt for typing the manuscript.

References

1 D. L. Hughes, M. Y. Mohammed, and C. J. Pickett, *J. Chem. Soc., Chem. Commun.*, 1989, 1399.
2 M. Y. Mohammed and C. J. Pickett, *J. Chem. Soc., Chem. Commun.*, 1988, 1119.
3 D. L. Hughes, M. Y. Mohammed, and C. J. Pickett, *J. Chem. Soc., Chem. Commun.*, 1988, 1481.
4 D. L. Hughes, D. J. Lowe, M. Y. Mohammed, C. J. Macdonald, and C. J. Pickett, *Polyhedron*, 1989, **8**, 1653.
5 J. Chatt and J. R. Dilworth, *J. Indian Chem. Soc.*, 1977, **54**, 13; *J. Chem. Soc., Chem. Commun.*, 1975, 983.
6 P. C. Bevan, J. Chatt, J. R. Dilworth, R. A. Henderson, and G. J. Leigh, *J. Chem. Soc., Dalton Trans.*, 1982, 821.
7 J. Schmitte, C. Friebel, F. Weller, and K. Dehnicke, *Z. Anorg. Allg. Chem.*, 1982, **495**, 148.
8 J. Strähle, U. Weiher, and K. Dehnicke, *Z. Naturforsch., Teil B*, 1978, **33**, 1347.
9 M. W. Bishop, J. Chatt, J. R. Dilworth, M. B. Hursthouse, and M. Motevalli, *J. Chem. Soc., Chem. Commun.*, 1976, 780
10 U. Müller, R. Kujanek, and K. Dehnicke, *Z. Anorg. Allg. Chem.*, 1982, **495**, 127.
11 T. Godemeyer, E. Weller, K. Dehnicke, and D. Fenske, *Z. Anorg. Allg. Chem.*, 1987, **554**, 92.
12 J. R. Dilworth, P. L. Dahlstrom, J. R. Hyde, and J. Zubieta, *Inorg. Chim. Acta*, 1983, **71**, 21.
13 J. Chatt, R. Choukroun, J. R. Dilworth, J. R. Hyde, P. Vella, and J. Zubieta, *Transition Met. Chem. (Weinheim, Ger.)*, 1979, **4**, 59.
14 M. W. Bishop, J. Chatt, J. R. Dilworth, B. D. Neaves, P. Dahlstrom, J. Hyde, and J. Zubieta, *J. Organomet. Chem.*, 1981, **213**, 109.
15 W. Hussain, G. J. Leigh, H. Modh. Ali, C. J. Pickett, and D. A. Rankin, *J. Chem. Soc., Dalton Trans.*, 1984, 1703.

16 A. Galindo, A. Hills, D. L. Hughes, and R. L. Richards, *J. Chem. Soc., Chem. Commun.*, 1987, 1815; A. Galindo, A. Hills, D. L. Hughes, and R. L. Richards, M. Hughes, and J. Mason, *J. Chem. Soc., Dalton Trans.*, 1990, 283; G. J. Leigh, personal communication.
17 G. M. Sheldrick, SHELX 76, Program for crystal structure determination, University of Cambridge, 1976.
18 G. M. Sheldrick, Program SHELXS, in 'Crystallographic Computing 3,' eds. G. M. Sheldrick, C. Krüger, and R. Goddard, Oxford University Press, 1985, p. 175.
19 'International Tables for *X*-Ray Crystallography,' Kynoch Press, Birmingham, 1974, vol. 4, pp. 99 and 149.
20 S. N. Anderson, R. L. Richards, and D. L. Hughes, *J. Chem. Soc., Dalton Trans.*, 1986, 245.
21 F. T. Al-Ani and C. J. Pickett, *J. Chem. Soc., Dalton Trans.*, 1988, 2329.

Received 10*th November* 1989; *Paper* 9/04834K